HoxB genes regulate neuronal delamination in the trunk neural tube by controlling the expression of Lzts1

Axelle Wilmerding, Lucrezia Rinaldi, Nathalie Caruso, Laure Lo Re, Emilie Bonzom, Andrew J Saurin, Yacine Graba, Marie-Claire Delfini

HoxB genes regulate neuronal delamination in the trunk neural tube by controlling the expression of *Lzts1*

Axelle Wilmerding 1*, Lucrezia Rinaldi 1 2*, Nathalie Caruso 1, Laure Lo Re 1 3, Emilie Bonzom 1, Andrew J. Saurin 1, Yacine Graba 1 # ✉ and Marie-Claire Delfini 1 # ✉

1 Aix Marseille Univ, CNRS, IBDM, Marseille, France

2 Present address: Division of Translational Therapeutics, Department of Medicine and the Cancer Center, Beth Israel Deaconess Medical Center, Harvard Medical School, Boston, Massachusetts

3 Present address: King's college London,Wolfson Centre for Age-Related Diseases, London, United Kingdom

***** Co-first authors

Co-senior authors

✉ e-mail : yacine.graba@univ-amu.fr and marie-claire.delfini-farcot@univ-amu.fr

Running title: *HoxB* control neuronal delamination

Key words: Hox transcription factors, Lzts1, Spinal Cord Development, Neurogenesis, Delamination, Chicken embryo

Summary statement:

Atypical function of *HoxB* genes during spinal cord development: instead of giving positional information, HoxB regulate the delamination of the neuronally differentiating cells by controlling the expression of *Lzts1*.

ABSTRACT

Differential *Hox* gene expression is central for specification of axial neuronal diversity in the spinal cord. Here, we uncover an additional function of Hox proteins in the developing spinal cord, restricted to B cluster Hox genes. We found that members of the HoxB cluster are expressed in the trunk neural tube of chicken embryo earlier than Hox from the other clusters, with poor antero-posterior axial specificity and with overlapping expression in the intermediate zone (IZ). Gain-of-function experiments of HoxB4, HoxB8 and HoxB9, respectively representative of anterior, central, and posterior *HoxB* genes, resulted in ectopic progenitor cells in the mantle zone. The search for HoxB8 downstream targets in the early neural tube identified the Leucine Zipper Tumor Suppressor 1 gene (*Lzts1*), whose expression is also activated by HoxB4 and HoxB9. Gain and loss of function experiments showed that Lzts1, expressed endogenously in the IZ, controls neuronal delamination. These data collectively indicate that *HoxB* genes have a generic function in the developing spinal cord, controlling the expression of *Lzts1* and neuronal delamination.

INTRODUCTION

Hox genes encode highly conserved homeodomain (HD) transcription factors essential to promote morphological diversification of the bilaterian body (Rezsohazy et al., 2015). In higher vertebrates including humans, mice and chicken, 39 *Hox* genes specify the regional identity of body structures including the axial skeleton, nervous system, limbs, genitalia, and the intestinal and reproductive tracts (Crawford, 2003). *Hox* genes are organized in 4 clusters located on different chromosomes named *HoxA* to *HoxD*, and in 13 paralog groups. Members of each paralog group, further classified in anterior, central and posterior classes, are deployed in ordered spatial and temporal patterns along the antero-posterior (AP) axis (Duboule, 2007; Duboule and Dollé, 1989; Iimura and Pourquié, 2006; Pearson et al., 2005). Genes located 3' in a cluster are expressed earlier and more rostral than genes located more 5'. The correlation between the genomic organization and the spatio-temporal characteristics of Hox gene expression along the AP body axis is referred to as "collinearity". Importantly, genes of the same paralog group, including in distant species, display higher sequence conservation and regulatory properties than different paralogs within the same species. Together with the collinear expression, this results in the deployment of distinct regulatory activities in distinct spatial territories, allowing for morphological diversification.

The expression and function of Hox genes in the developing spinal cord of vertebrates (the trunk neural tube) illustrate how Hox collinear expression generates morphological diversification. From a functional point of view, experimental evidence showed that Hox genes define the identity and synaptic pattern of neurons, setting distinctive features necessary for the building of locally distinct motor circuits ultimately controlling diverse functions such as locomotion or respiration (Dasen et al., 2003, 2008; Lacombe et al., 2013; Sweeney et al., 2018). Hox gene functions in the trunk neural tube include the segregation of motor neurons columns: LMC (lateral motor column) in a ventrolateral position at limb levels (brachial and lumbar levels), PGCs (preganglionic motor column) and HMCs (hypaxial motor neurons) at the thoracic level. This neuron segregation according to their final functions is essential for subsequent functional organization of the spinal cord.

Previous studies provided an extensive view of Hox gene expression in the chicken and mouse trunk neural tube (Dasen et al., 2005; Jung et al., 2010; Lacombe et al., 2013). The expression of HoxA, HoxC and HoxD genes display a pronounced axial collinearity, with in most cases a preferential accumulation in motor neuron territories after the onset of neuronal

differentiation, which suits the described pattern of activity of Hox genes in promoting motor neuronal diversification.

Available data on HoxB genes suggest expression with distinct levels of axial collinearity. HoxB genes start to be expressed very early in the embryo (in the epiblast/tailbud), and present a temporal collinear onset of expression: HoxB1 and HoxB2 at HH4, HoxB3 to HoxB6 at HH5, HoxB7 at HH6, HoxB8 and HoxB9 at HH7, and HoxB13, only expressed in the tail bud, at HH20 (Denans et al., 2015). In the trunk neural tube of chicken embryo from HH4 to HH17, HoxB genes can be split into two groups: HoxB1 to HoxB5 are expressed up to the otic vesicle but not in the caudal part, while HoxB6 to HoxB9 are expressed in the caudal part of the neural tube (Bel-Vialar et al., 2002). The exhaustive view of the expression of Hox genes and proteins much later (at E6) in the trunk neural tube shows in contrast that at later stages the expression of all HoxB genes is highly overlapping along the antero-posterior axis : HoxB3 to HoxB9 genes are all expressed at the brachial, thoracic and lumbar level (Dasen et al., 2005). In addition, at E6, Hox from the B cluster display an almost complete absence of expression in motor neurons, where Hox from the other clusters (HoxA, HoxC and HoxD) display a strong collinear expression to specify columnar and pool subtypes (Dasen et al., 2005). Although less comprehensive, data in mouse are also consistent with B cluster Hox genes displaying characteristics of expression distinct from non-B cluster Hox genes (Graham et al., 1991; Jung et al., 2010; Lacombe et al., 2013). These observations indicate a different spatial deployment of B cluster Hox genes. Interestingly, HoxB8 protein is present in chicken neural tube progenitors (Asli and Kessel, 2010), thus, long before the expression of non-B cluster Hox proteins. Early transcription at the progenitor stage of non-B cluster Hox genes were described, but their proteins are either weakly expressed or undetectable, with proteins observed only in postmitotic neurons (Dasen et al., 2003). Therefore, HoxB genes may have earlier functions than non-B Hox genes in the trunk neural tube development.

The trunk neural tube is a pseudostratified epithelium that will sequentially give rise to a large variety of neurons and glial cells of the spinal cord. After an initial phase of proliferation resulting in the expansion of progenitors by symmetrical divisions (P-P), neurogenesis and then gliogenesis are achieved via a succession of steps that follow a stereotypic temporal order. Concomitantly, progenitors become committed to differentiate into a specific neuronal (and later on glial) subtype according to their dorso-ventral position (Le Dréau and Martí, 2012). Postmitotic neurons (N) are produced by asymmetric (P-N) or symmetric terminal (N-N) divisions of progenitor cells (Götz and Huttner, 2005). As neural

tube cells progress through the cell cycle, they undergo interkinetic nuclear migration with nuclei undergoing mitosis at the ventricular surface of the neural tube (at the apical part of the cells, close to the lumen of the neural tube) while their daughter cells reach the G1/S checkpoint as nuclei reach the basal limit of the progenitor zone, where they either re-enter or exit the cell cycle (Lee and Norden, 2013). Post-mitotic cells remain at the lateral face of the neural tube where they contribute to the mantle zone (MZ) and acquire further differentiated features. Therefore, as neurogenesis progresses, the MZ thickens. The intermediate layer between the progenitor area (or ventricular zone (VZ) and the MZ, called intermediate zone (IZ), contains the newly born neurons on their way to their final position (Corral and Storey, 2001).

The progenitors/neurons ratio is controlled by the proliferation properties of progenitors (length and rounds of cell cycles), by the survival of progenitors and differentiating neurons, and by progenitor cell fate decisions (to remain a progenitor or to differentiate). Progenitor cell fate decisions are based on the activation of a cascade of transcription factors triggered by proneural genes (Bertrand et al., 2002; Lacomme et al., 2012; Ma et al., 1996), whose expression is largely controlled by the Notch signaling pathway (Formosa-Jordan et al., 2013; Hatakeyama, 2004; Hatakeyama et al., 2006). The mediolateral spatial organization of the differentiating neural tube into the three layers (VZ, IZ, MZ) is important for ensuring a proper differentiation rate since in the nascent IZ neurons, proneural genes induce the expression of Notch ligands such as Delta1 and Jagged which in turn activate Notch1 that down-regulates proneural gene expression and inhibits neurogenesis in neighboring precursors. Correct spatial organization of the neural tube along the medio-lateral axis requires timely detachment of newborn neurons from the apical surface in order to exit this proliferative zone and begin the morphological reorganization that underlies neuronal differentiation. This apical detachment process is known as delamination (Kasioulis and Storey, 2018). While it has been recently shown that the synchronization of the delamination is controlled by Notch pathway (Baek et al., 2018), molecular mechanisms controlling the timing of the delamination are not fully understood.

In this study, we aimed at investigating the function of B cluster Hox genes at early steps of trunk neural tube development using the chicken embryo as a model from E2 stage onwards when non-B Hox genes are not yet expressed, and prior to the well-documented role of Hox genes in motor neuron differentiation.

RESULTS

HoxB genes are expressed early in the trunk neural tube during neurogenesis with little antero-posterior axial specificity

Numerous studies have described *Hox* gene expression in the trunk neural tube of chicken embryo. The lack of marked axial specificity of the *HoxB* genes within the brachial, lumbar and sacral territories of the trunk neural tube at E6, with an expression profile very different from the *Hox* genes of other clusters (Dasen et al., 2005) prompted us to re-investigate the expression and function of B cluster Hox genes during early spinal cord development.

We started by exploring *HoxB* expression patterns between E3 and E5 in the trunk neural tube using whole mount and transverse section *in situ* hybridizations for anterior (*HoxB2*, *HoxB4*), central (*HoxB5*, *HoxB7* and *HoxB8*) and posterior (*HoxB9*) classes of *Hox* genes. As early as E3, *HoxB* genes are expressed in largely overlapping territories, from the neck (in which, however, there is still a weak spatial collinearity) to the tail (Fig. 1A and B). In addition to highlighting the large overlap in the spatial expression domains of *HoxB* genes (except *HoxB13* which is only expressed in the tail bud after stage HH20 (Denans et al., 2015)), our results confirm that *HoxB* transcripts are present in the trunk neural tube before the onset of neurogenesis (Fig. 1A and B). To assess the presence of HoxB proteins in the trunk neural tube, including at early stages, we raised an antibody specific to the posterior HoxB9 protein (Supplementary Fig. 1 displays the specificity of the HoxB9 antibody). Immunostainings with this antibody on transverse sections show that HoxB9 protein is present in the trunk neural tube as early as E3 (Fig. 1C) and is broadly expressed from the neck to the tail (Fig. 1D) (coincident with *HoxB9* transcripts (Fig. 1A)). This contrasts with its paralog HoxC9 protein, not yet expressed at E3 in the neural tube (Fig. 1C), expressed only later and only at the thoracic level (Fig. 1D). *In situ* hybridization with the *HoxB8* probe (a similar pattern was described for the HoxB8 protein (Asli and Kessel, 2010)), and immunostaining with the HoxB9 antibody on the same transverse sections at E4.5 highlight the strong overlap in the expression of these “central” and “posterior” HoxB members, along the antero-posterior axis of the chicken embryo, from cervical to sacral level (Fig. 1E).

Altogether, our expression data define a temporal and spatial time window that differs from non-B cluster *Hox* genes. The lack of clear axial specificity does not favor a role for *HoxB* genes in an antero-posterior axial diversification of the neural tube, but HoxB early and

broad expression rather suggest a generic function during neurogenesis of the developing trunk neural tube.

***HoxB* gene expression in the trunk neural tube resolves in the IZ and controls early neurogenesis**

The comparison of the expression pattern of *HoxB* genes with markers of the three layers of the trunk neural tube (Sox2 for the VZ, *NeuroD4* for the IZ, and Tuj1 for the MZ) at E4 (Fig. 2A), shows that in addition to disappearing from the differentiating motor neuron domain where non-B cluster *Hox* genes are expressed, *HoxB* gene and protein expression at that stage is mainly restricted in the IZ, although weak expression is observed in the VZ (Fig. 1C-E, Fig. 2A and Supplementary Fig. 2). These expression dynamics suggest that *HoxB* genes, although not exclusively, may control neurogenesis progression by controlling the expression of genes expressed in the IZ. As *HoxB* genes are expressed in the IZ all along the dorso-ventral axis, and from the neck to the tail (Fig. 1C-E), this function would apply to all neuronal subtypes, i.e. motor neurons and all interneurons, and this, irrespective of the antero-posterior axial position (except in the neck) and of the paralog identity of the *HoxB* gene.

The largely overlapping HoxB expression patterns suggest *HoxB* gene functional redundancy which compromises loss of function approaches. We thus probed the function of *HoxB* genes in neural tube development by gain-of-function experiments. HoxB4, HoxB8 and HoxB9 were chosen as representative of anterior, central, and posterior *HoxB* genes respectively. Neural tubes of E2 embryos were unilaterally electroporated with a control plasmid encoding GFP or with each HoxB expression vector co-expressing GFP (to report transfected cells). Immunostainings were performed with antibodies against the progenitor marker Sox2 and the pan-neuronal marker Tuj1. Results show the presence of ectopic Sox2 positive cells in the MZ on the electroporated side for all three *HoxB* gene gain-of-function experiments at either two (Supplementary Fig. 3) or three days (Supplementary Fig. 4) after electroporation. We observed the ectopic Sox2 phenotype at all dorso-ventral positions in the spinal cord (Supplementary Fig. 4). The phenotype obtained is however modest, with only a few ectopic Sox2 positive cells in the MZ. The low penetrance of the phenotype could result from elimination of ectopic Sox2 cells by apoptosis, a hypothesis consistent with increased apoptosis following HoxB8 electroporation (Supplementary Fig. 5). The hypothesis was probed by analyzing embryos co-transfected with HoxB (HoxB4, HoxB8 or HoxB9) and P35 (an inhibitor of apoptosis (Sahdev et al., 2010)) expression vectors. Quantification of Sox2

ectopic cells in the MZ 72 hours after HoxB4, HoxB8 and HoxB9 gain-of-function in the context of P35 expression shows a strong phenotype (around 35% of transfected cells (GFP+) in the MZ are Sox2 positive after the overexpression of any of the three HoxB). Ectopic Sox2 cells in the MZ are rarely seen under control condition (control vector + P35) (Fig. 2C). These results indicate that cell elimination through apoptosis contributes to the modest phenotype observed in HoxB gain of function experiments, and that the full range of HoxB induced phenotype can only be observed when suppressing apoptosis.

The phenotypes triggered by each of the three HoxB genes' overexpression are similar, with no marked differences in their potential to induce ectopic Sox2 positive cells (Fig. 2C) The phenotype of HoxB gain-of-function is not strictly cell-autonomous since Sox2 positive GFP negative can be found in the MZ (Fig. 2D). In addition, Sox2/pH3 and Sox2/EdU double-staining following HoxB8 gain-of-function shows that Sox2 ectopic cells in the MZ are still mitotic (Fig. 2D and Supplementary Fig. 6), a characteristic of progenitor cells.

We conclude from this set of experiments that HoxB genes, irrespective of their paralog identity, induce when overexpressed a similar phenotype consisting of the appearance of ectopic progenitors (Sox2 positive) cells in the MZ. Taken together with expression pattern data, this suggests a generic role for HoxB genes in the control of early neural tube differentiation (neurogenesis and/or neuronal delamination). We next questioned if non-B Hox genes, while not expressed at these early stages, also have the capacity to induce ectopic Sox2 cells in the MZ. The hypothesis was probed by forcing the premature expression of HoxA7, HoxC8 and HoxD8 (one representative of each non-HoxB cluster Hox) from E2 (these experiments were done in a P35 context). Results showed that such an expression leads to a phenotype similar (ectopic Sox2 cells in the MZ) to those exhibited by B cluster Hox genes (Supplementary Fig. 7), supporting that the induction of ectopic Sox2 cells in the MZ is a regulatory property also embedded in non-B Hox proteins.

Transcriptomic data identifies *Lzts1* as a target of HoxB8

To get molecular insights into HoxB gene function in the early neural tube, we aimed to identify downstream target genes of the HoxB transcription factors, focusing on the central class HoxB8 protein. E2 neural tubes were bilaterally electroporated with either a control vector encoding nuclear GFP (pCIG) or a HoxB8 expression vector co-expressing nuclear GFP (pCIG-HoxB8) (Fig. 3A). The regions of the neural tube expressing the GFP were

dissected 18 hours after electroporation and dissociated. GFP-expressing cells were isolated by FACS with the use of a dead cell exclusion (DCE)/discrimination dye (DAPI) to eliminate dying cells (Supplementary Fig. 8). Two independent RNAs samples were extracted, reverse transcribed, and cDNAs were amplified using a linear amplification system and used for sequencing library building. Qualitative analysis of RNA-seq data from the two biological replicates shows a high pearson correlation score (>0,98) indicative of the experimental reproducibility (Supplementary Fig. 9). RNA-seq data from aligment to the Galgal4 genome assembly identified 1913 genes with significantly changed expression (Fig. 3B FDR5 (False Discovery Rate 5), Table 1 and Table 2; see also Material and Methods section), of which 1,097 were up-regulated (57%) (Table 1) and 816 down-regulated (43%) (Table 2) (Fig. 3C left panel). This tendency of HoxB8 to act as activator rather than repressor is amplified when selecting genes differentially expressed by more than two-fold, with 251 being up-regulated (90%) and only 25 down-regulated (10%) (Fig. 3C right panel). Gene ontology enrichment analysis (GOEA) of the biological processes suggests pleiotropic functions of HoxB8 during spinal cord development (Fig. 3D and Table 3) including neuron differentiation, apoptotic process, cell cycle and cell migration (Fig. 3D). In particular, the Notch signaling pathway, a key regulator of neurogenesis (Formosa-Jordan et al., 2013; Hatakeyama, 2004; Hatakeyama et al., 2006), stands out from the GOEA (Fig. 3D – downregulated genes), suggesting that HoxB8 controls neurogenesis. This is illustrated by Hes5.1, a Notch pathway effector expressed in the VZ and known to keep neural tube cells in a progenitor state (Fior and Henrique, 2005), for which transcripts *in situ* hybridization shows strong transcriptional downregulation (Supplementary Fig. 10, Table 1).

Among all deregulated genes, the Leucine zipper tumor suppressor 1 (*Lzts1*) gene (also known as FEZ1 and PSD-Zip70) (Baffa et al., 2008; Ishii et al., 2001; Vecchione et al., 2007) caught our attention for two reasons. First, Lzts1, upregulated by HoxB8 (Fig. 3B,E and Table 1) is, as HoxB, preferentially expressed in the IZ in the trunk neural tube of chicken and mouse embryos (Kropp and Wilson, 2012). Second, Lzts1 has been recently shown to control neuronal delamination during mammalian cerebral development (Kawaue et al., 2019), a function that if conserved in the neural tube, could account for the HoxB-induced ectopic Sox2 positive cells found in the MZ.

We studied the dynamics of *Lzts1* expression by *in situ* hybridizations with an *Lzts1* probe at E2, E3 and E4 stages (Fig. 4A-B and Supplementary Fig. 11). At E3, *Lzts1* transcripts are already found in the IZ, which, due to the lack of differentiated neurons that will form the MZ at that stage, is in the most lateral region of the neural tube (Fig. 4A). At E4,

as previously described (Kropp and Wilson, 2012), *Lzts1* transcripts are still associated with the IZ, located between progenitors of the VZ and differentiated neurons of the MZ (Supplementary Fig. 11B), with an expression pattern very similar to HoxB genes (Fig. 4B and Supplementary Fig. 12). Indeed, while not completely overlapping since HoxB are still expressed in the VZ at low level, *Lzts1* transcripts are enriched where the HoxB9 protein level is the highest (Supplementary Fig. 12). The expression of *Lzts1* gene is not restricted to a specific antero-posterior region of the neural tube (Supplementary Fig. 11A and Supplementary Fig. 12). The *Lzts1* expression pattern is thus compatible with a regulation by HoxB proteins in the IZ. Consistent with its identification as a HoxB8 target in the transcriptomic approach, *in situ* hybridization with an *Lzts1* probe following HoxB8 gain-of-function shows ectopic *Lzts1* expression in the trunk neural tube (Fig. 4C). If *Lzts1* regulation illustrates at the level of a single target the generic control of early neurogenesis documented in Fig. 2, HoxB4 and HoxB9 should also induce ectopic *Lzts1* expression, which is indeed observed (Fig. 4C). Lzts1 transcriptional activation is faint, consistent with the 2.7-fold transcript enrichment seen in the RNA-seq data, and is mainly observed in the ventricular zone (Fig. 4). Co-expressing HoxB4, HoxB8 or HoxB9 with the P35 apoptotic inhibitor does not allow for stronger and more frequent Lzts1 induction, in particular in the MZ, where in such conditions the frequency of Sox2 positive cells in the MZ is high. This indicates that the lack of Lzts1 induction in cells of the MZ, is not due to cell elimination by apoptosis, suggesting that HoxB proteins can only transcriptionally control *Lzts1* expression within a sharp time window, when cells are still in the VZ or IZ.

We also found that HoxA7, HoxC8 and HoxD8 gain-of-functions induce *Lzts1* expression (Supplementary Fig. 14), showing that as in the case of Sox2 ectopic cells induction in the MZ, Lzts1 transcriptional activation by Hox proteins relies on regulatory properties embedded in B and non-B Hox proteins. These results show that *Lzts1*, identified as a HoxB8 target, is a generic Hox target. However, only B cluster Hox genes are expressed at the proper time and space for assuming that function.

Lzts1 controls the delamination of newborn neurons in the trunk neural tube

Premature delamination of neural progenitors may explain the presence of ectopic Sox2 cells in the MZ after the HoxB gain-of-functions. The function of *Lzts1* in neuronal development within the trunk neural tube is not known, but it has been described to positively control neuronal delamination in brain development in mammalian (Kawaue et al., 2019). Due to its

expression in the IZ, where progenitors switch to neurons and lose their apical attachment, Lzts1 may also control delamination during spinal cord neurogenesis.

To examine this, we analyzed the consequences of Lzts1 gain-of-function, obtained through unilateral electroporation of an Lzts1 expression vector in the neural tube at E2 (Supplementary Fig. 15). The tracking of the cytoplasmic GFP demonstrated massive cell delamination with nearly all electroporated cells losing their attachment to the lumen and found in the MZ (Fig. 5A). This phenotype is seen both at two and three days after electroporation (Fig. 5A). Under normal conditions, only newborn neurons lose their apical attachment (Kasioulis and Storey, 2018) suggesting that Lzts1 in the IZ is involved in the control of newborn neuron delamination. Immunostainings with Sox2 and Tuj1 antibodies (progenitor and neuronal markers, respectively) (Fig. 5 and Supplementary Fig. 16) showed that nearly half (47,7%) of the Lzts1 gain-of-function cells in the MZ ectopically express Sox2 (Fig. 5C). This suggests that Lzts1 gain-of-function forces the delamination but not neural differentiation, since cells which prematurely delaminate stay in a progenitor state (Fig. 5B-C). This is distinct from Neurogenin2 gain-of-function where electroporated cells massively delaminate but also prematurely differentiate. (Garcia-Gutierrez et al., 2014). The Lzts1 delamination “only” phenotype is confirmed by the finding that the MZ ectopic Sox2 positive cells keep progenitor characteristics: they express CCND1/CyclinD1 (Fig. 5D) and the pH3 mitotic marker (Fig. 5E), and Hes5.1 and NeuroD4 genes respectively markers of the VZ and IZ (Fig. 5F, G). The phenotype induced by Lzts1 gain-of-function is independent of the dorso-ventral and antero-posterior position within the trunk neural tube (Fig. 5B and Supplementary Fig. 16) and is not strictly cell-autonomous (ectopic Sox2 positive GFP negative cells can be found following Lzts1 gain of function; Supplementary Fig. 16).

To support conclusion from Lzts1 gain-of-function experiments, we analyzed the effects of Lzts1 loss-of-function. Knockdown was obtained through unilateral electroporation of a ShRNA expressing plasmid at E2. The efficiency of the ShRNA was assessed by following *Lzts1* transcripts (Fig. 6A), showing a strong effect illustrated by the absence of the typical *Lzts1* expression in the IZ. The effects of *Lzts1* knockdown were studied using the Sox2 progenitor (Fig. 6B) and Tuj1 or HuC/D (Fig. 6C-F, Supplementary Fig. 17) neuronal markers. Results show that Lzts1 knockdown does not lead to ectopic Sox2 cells as induced by Lzts1 gain-of-function, but instead leads to an ectopic expression of Tuj1 or HuCD neuronal markers in the VZ with neurons keeping their apical attachment (Fig. 6C-F). The loss-of-function of *Lzts1* thus results in neuronal delamination inhibition, a phenotype that

mirrors the promotion of neuronal delamination seen in Lzts1 gain-of-function experiments (Fig. 5 and Supplementary Fig. 16).

Collectively, Lzts1 gain and loss of function experiments demonstrate a role for Lzts1 in controlling neural delamination in the trunk neural tube. As impaired delamination is a plausible explanation for the generic HoxB-induced MZ ectopic Sox2 cells, and as *Lzts1* transcripts are induced by HoxB proteins, Lzts1 is likely to be a key HoxB effector leading to the MZ ectopic Sox2 phenotype. To probe this hypothesis, we performed epistatic experiments by co-expressing HoxB8 and the ShRNA-Lzts1 ShRNA, in the P35 context so to start with a stronger HoxB induced phenotype. Results show that Lzts1 gene inactivation lowers significantly the occurrence of Sox2 ectopic cells in the MZ (Fig. 6 G-I), supporting that Lzts1 is a key effector in the HoxB induced delamination phenotype.

DISCUSSION

A broad B-cluster specific function for Hox genes in early spinal cord development

Our work extends the functional contribution of Hox genes to spinal cord development. While largely shown to act as "choreographers" of neural development in specifying motor neurons subtypes (Philippidou and Dasen, 2013), this study highlights an unexpected early and general role in controlling early neurogenesis and neuronal delamination. Previous expression data delineated that B cluster *Hox* gene expression at E6, a stage when motor neuron subtypes are defined, does not follow axial collinearity, as non-B cluster Hox genes do, and are generally excluded from differentiating motor neurons (Dasen et al., 2005; Jung et al., 2010; Lacombe et al., 2013). Based on the expression analysis of representatives of anterior, central and posterior Hox paralogs, we propose that B cluster Hox genes (excepted HoxB13) are expressed in the chicken neural tube earlier than non-B cluster Hox genes, in a largely ubiquitous pattern that later resolves in preferential expression in the IZ, the region of the trunk neural tube where neuronal progenitors exit the cell cycle and delaminate to transit toward the mantle zone. Consistent with the lack of axial collinearity already observed at E6, B cluster Hox gene expression displays little axial specificity, with most HoxB genes expressed in largely overlapping expression patterns in the trunk neural tube (Figure 7). These expression patterns suggest a function distinct from endowing the neural tube with axial positional information required for proper setting of neuronal subtype along the AP axis, well

documented for *Hox* A, C and D genes. It rather suggests that B cluster Hox genes act without paralog specificity all along the trunk neural tube, in a “generic” manner, giving a temporal instead of positional information. While long underseen, a recent literature survey indicates that such generic functions are constitutive of Hox protein function (Saurin et al., 2018), and may be an intrinsic deeply rooted property of Hox proteins reflecting their phylogenetic common origin. An illustration of such a function is the generic control of autophagy by Hox proteins in the Drosophila fat body (Banreti et al., 2014), where as seen here in the chicken neural tube, Hox genes are broadly expressed in the tissue. A difficulty to study such generic function, which has contributed to its late recognition, is that revealing them can often not be achieved by conventional loss-of-function approaches, as mutating one or even a few Hox genes does not alter the shared generic function, due to inter-paralog functional compensation (Banreti et al., 2014).

To get insights into early B cluster Hox gene function in the chicken neural tube, we thus took a gain-of-function approach. Results obtained indicate that Hox gain-of-function results in the appearance of progenitor Sox2 positive cells in the MZ, a region of the neural tube that normally hosts differentiated post-mitotic neurons. Consistent with a shared “generic” function suggested by the expression patterns, we found that anterior, central and posterior HoxB genes induce similar defects, all resulting in ectopic Sox2 positive cells in the MZ. This phenotype is observed all along the trunk neural tube and occurs at all dorso-ventral positions within the tube, indicating that this generic Hox function may be relevant to neurogenesis progression in general, irrespective of the final antero-posterior or dorso-ventral driven final neuronal identity. We also found that gain-of-function experiments conducted with the non-B proteins HoxA7, HoxC8 and HoxD8, not expressed at early stage in the neural tube, also result in ectopic Sox2 positive cells in the MZ. This suggests that the control of the process leading on the Sox2 positive cells in the MZ is a regulatory property likely embedded into Hox proteins in general, and may rely on the similar biochemical characteristics of Hox proteins, with most Hox proteins displaying similar DNA binding properties (Hayashi and Scott, 1990; Mann and Chan, 1996; Mann et al., 2009; Merabet and Mann, 2016; Zandvakili and Gebelein, 2016). The B cluster specificity would thus arise strictly from the temporal and spatial deployment of B cluster proteins, and not from intrinsic properties specific to B cluster Hox proteins. In agreement with this hypothesis, in silico survey of sequence conservation in Hox proteins, including short linear motifs (SLiMs), does not reveal any characteristics specific to the B cluster Hox proteins (Rinaldi et al., 2018).

Insights into HoxB generic function from the study of the *Lzts1* downstream target

To circumvent the difficulty of gaining functional insights into HoxB gene function in the early chicken neural tube from loss-of-function approaches, we reasoned that identifying and studying HoxB downstream targets, including through loss-of-function approaches, would allow assessing better how HoxB genes influence early spinal cord development. Transcriptomic data obtained one day after HoxB8 overexpression highlights genes and pathways well known to control multiple aspects of neurogenesis including Notch and IGF pathway effectors (Fior and Henrique, 2005; Fishwick et al., 2010; Vilas-Boas and Henrique, 2010), suggesting that HoxB gene influence on early neurogenesis is diverse. For this study we focused on *Lzts1*, which shares with HoxB genes a preferential expression in the IZ, the region of the trunk neural tube containing the newly born neurons on their way to their final position (the MZ), and thus may account for the main phenotype (Sox2 ectopic cells in the MZ) seen in HoxB overexpression experiments.

The study of Lzts1 gain and loss-of-function experiments showed that *Lzts1* controls the delamination of newborn neurons: gain-of-function induces massive cell delamination with nearly all electroporated cells losing their attachment to the lumen and found in the MZ, while loss-of-function leads to differentiated neurons keeping their apical attachment. The promotion of delamination by Lzts1 further suggests that the appearance of Sox2 positive cells in the MZ, seen in Lzts1 and Hox gain-of-function experiments, results from loss of apical attachment and subsequent migration of progenitor Sox2 positive cells in the MZ. Consistent with the view that *Lzts1* mediates HoxB generic function in the chicken early neural tube, we observed that *Lzts1* expression is influenced not only by HoxB8, but also by all other HoxB cluster genes probed (the anterior HoxB4 and posterior HoxB9 class genes), and that Lzts1 gene knockdown in a HoxB8 gain-of-function experiment significantly lowers the HoxB8-induced ectopic Sox2 phenotype. Although both HoxB and Lzts1 overexpression result in ectopic Sox2 positive cells in the MZ, the HoxB overexpression phenotypes are less pronounced than *Lzts1* gain-of-function (including in a P35 context which inhibits cell death), with fewer ectopic Sox2 positive cells seen in the MZ. This weaker phenotype is in line with the limited capacity of HoxB genes to induce *Lzts1* expression in gain-of-function experiments, which likely reflects a sharp time window within which *Lzts1* transcriptional activation by HoxB proteins is possible.

HoxB and Lzts1 function in the IZ might be conserved in higher vertebrates

HoxB control of neural delamination via the regulation of *Lzts1* in the IZ uncovered by this study might be shared by higher vertebrates. Expression patterns of the *HoxB* and *Lzts1* genes in the trunk neural tube of mouse embryo are highly reminiscent of chicken embryo: *Lzts1* is also expressed in the IZ (Kropp and Wilson, 2012); *HoxB* genes, also expressed earlier than non-B cluster *Hox* genes, also have a broadly overlapping expression in the neural tube and are also excluded from the motor neuron area as in chicken (Graham et al., 1991; Jung et al., 2010; Lacombe et al., 2013). However, *HoxB* gene expression does not seem to resolve in the IZ as sharply as in the chicken. HoxB activity might be restrained to the IZ through the expression and action in the VZ of Geminin, a pleiotropic cell-cycle regulator also known to inhibits Hox protein (Luo et al., 2004; Patterson et al., 2014). In this situation, only cells that express *HoxB* genes laterally to the limit of Geminin expression, which corresponds to the IZ, would be free of the Geminin inhibitor and allow HoxB-mediated Lzts1 transcriptional activation.

Lzts1 function in the control of neural delamination has already been described in mammalians, in the context of the brain (cephalic neural tube) of mouse and ferret (Kawaue et al., 2019). Kawaue and colleagues demonstrate that Lzts1, which associates with microtubule components and is involved in microtubule assembly (Ishii et al., 2001), controls apical delamination of neuronally committed cells of the brain by altering apical junctional organization (Kawaue et al., 2019). Indeed, in neuronally differentiating cells of the brain, Lzts1 modulates the microtubule-actin-AJ system at the apical endfeet to evoke apical contraction and reduce N-cadherin expression (Kawaue et al., 2019). Molecular mechanisms by which Lzts1 controls delamination in the trunk neural tube might be the same as in the mammalian brain. However, Lzts1 upstream regulation has to be distinct, as the brain is known as a Hox-free territory.

In humans, expression of the *LZTS1* gene (also named *FEZ1*) is altered in multiple tumors (Ishii et al., 1999). LZTS1 tumor suppressor function has been attributed at least in part to its role in the control of mitosis progression (Vecchione et al., 2007) and in regulating the Pi3k/AKT pathway (He and Liu, 2015; Zhou et al., 2015). Since the Pi3k/AKT pathway is required for neuron production in the trunk neural tube in both mouse and chicken embryos (Fishwick et al., 2010), Lzts1 might also regulate neuronal production in the trunk neural tube by regulating the Pi3k/AKT pathway in addition to controlling delamination.

MATERIALS AND METHODS

Ethics statement

Experiments performed with non-hatched avian embryos in the first two thirds of embryonic development time are not considered animal experiments according to the Directive 2010/63/EU.

Chicken embryos

Fertilized chicken eggs were obtained from EARL les Bruyeres (Dangers, France) and incubated horizontally at 38°C in a humidified incubator. Embryos were staged according to the developmental table of Hamburger and Hamilton (HH) (Hamburger and Hamilton, 1992) or according to days of incubation (E).

In ovo electroporation and plasmids

Neural tube *in ovo* electroporations were performed around HH12. Eggs were windowed, and the DNA solution was injected in neural tube lumen. Needle L-shape platinum electrodes (CUY613P5) were placed on both sides of the embryo at trunk level (5 mm apart), with the cathode always at its right. Five 50 ms pulses of 25 volts were given unilateral (or bilateral for RNAseq experiments) at 50 ms intervals with an electroporator NEPA21 (Nepagene).

The plasmids used for the gain-of-function experiments co-express a cytoplasmic or nuclear GFP (pCAGGS and pCIG respectively, used alone as controls) and the coding sequence (CDS) of the gene of interest. Vector used are: pCIZ-HoxB4, pCIG-HoxB8, pCIG-HoxB9 and pCIG-HoxC8 (gifted by Olivier Pourquié), pCAGGS-P35 (gifted by Xavier Morin) and pCAGGS-Lzts1, pCAGGS-HoxA7, pCAGGS-HoxD8, pCAGGS-HoxB4 pCAGGS-HoxB8 and pCAGGS-HoxB9 (this study). The CDS of HoxA7 and HoxD8 (second isoform, 567 bp) were PCR amplified from chicken neural tube cDNA; the CDS of HoxB4, HoxB8 and HoxB9 were PCR amplified from the plasmids described above and the CDS of Lzt1 was amplified from pGEMT-Lzts1 (gifted by Dr. S. Wilson). All sequences were subcloned in the pCAGGS plasmid using In-Fusion HD Cloning Kit (Takara). RNA interference technology was used to inhibit *Lzts1*, with the pRFPRNAiC vector, which

contains an RFP reporter gene (Das et al., 2006) and insertion sites for two siRNAs in tandem. The two 22 nucleotide-long target sequences for the ShLzts1 plasmid were chosen using the design tool "siRNA Target Finder" (AAGGTCAACCTGTTAGAGCAGG and AACATCATGCAGTGTGCCATCA). A shscrambled-Lzts1 plasmid was designed as control (AGAAGAGTGTACGGTCGCAGTC and GCATGTTGAACCGCAATACACT).

All the plasmids used for electroporation were purified using the Nucleobond Xtra Midi kit (Macherey-Nagel). Final concentration of DNA delivered by embryo for electroporation is between 1 to 2µg/µl except for epistatic experiment perfomed with DNA solution at 2,5µg/µl due to technical constraints (Table 4).

Immunofluorescence and fluorescent in situ hybridization

Embryos were fixed in 4% buffered formaldehyde in PBS then treated with a sucrose gradient (15% and 30% in PBS), embedded in OCT medium and stored at -80°C. Embryos were sectioned into 16 µm sections with a Leica cryostat and the slides were conserved at – 80°C or directly used for FISH and/or immunofluorescence.

Immunofluorescence

Slides were rehydrated in PBS then blocked with 10% goat serum, 3% BSA, 0,4% Triton X-100 in PBS for one hour. Primary antibodies were incubated over-night diluted in the same solution at 4°C. The following primary antibodies were used in this study: chicken anti-GFP 1:1000 (1020 AVES), rabbit anti-SOX2 1:500 (AB5603 Merck Millipore), mouse anti-Tuj1 1:500 (801202 Ozyme), mouse anti-HuC/D 1: 200 (Thermofischer 16A11), rat anti-pH3 1: 250 (S28, abcam ab10543), rabbit anti-Caspase 3 1:500 (Asp175, CST 9661), guinea pig anti-HoxC9 antibody 1:1000 (NY1638, gifted by Jeremy Dasen) and rabbit anti-LZTS1 1:250 (Sigma HPA006294). Polyclonal HoxB9 antibodies were raised in guinea pig using the peptide "143-158 GIVSNQRPSFEDNKVC" and used at 1:500. The secondary antibodies used were: anti-chicken, anti-rabbit, anti-mouse, anti-rat or anti-guinea pig conjugated with fluorochromes (488, 568 or 647) at 1:500. They were incubated for one hour in the blocking solution containing Hoechst (1:1000). Slides were washed, mounted (Thermo Scientific Shandon Immu-Mount) and imaged with a Zeiss microscope Z1 equipped with Apotome or a confocal LSM 780.

EdU labelling and detection

Proliferative cells were labelled with EdU using the Click it EdU Alexa Fluor 647 kit (Thermofisher). 400µl of a 0.5mM EdU solution (in PBS) was applied on top of the embryo and incubated at 38°C for 30mn. Cryostat sections were stained for EdU using manufacturer instructions.

Fluorescent in situ hybridization

The slides were treated with proteinase K 10 µg/ml (3 minutes at 37°C) in a solution of TrisHCl 50 mM pH 7.5, then in triethanolamine 0.1M and 0.25% acetic anhydride. They were pre-incubated with hybridization buffer (50% formamide, SCC 5X, Denharts 5X, yeast tRNA 250 µg/ml and herring sperm DNA 500 µg/ml) for 3h at room temperature, and incubated in the same buffer with DIG-labelled RNA probes over-night at 55°C in a wet chamber. The slides were then washed twice with 0.2X SCC for 30 minutes at 65°C. After 5 minutes in TNT buffer (100 mM Tris pH7.5, 150mM NaCl and 0.1% Tween-20), they were then blocked for 1h in buffer containing TNT 1X, 1% Blocking reagent (Roche) and 10% goat serum, then incubated in the same buffer for 3h with anti-DIG-POD antibodies (1:500, Roche) and revealed using the kit TSA-Plus Cyanin-3 (Perkin Elmer). RNA probes used for *in situ* hybridization were: *Lzts1, Hes5.1, Ccnd1, NeuroD4, HoxB4, HoxB5, HoxB7, HoxB8 and HoxB9*. The plasmids used to generate the *Hox* RNA probes were gifts from Jeremy Dasen and Olivier Pourquié (except *HoxB8 –PCR primer forward:* `CCAGCTCCCCTTACCAACAG` *and T7 reverse:* `TAATACGACTCACTATAGGGCCTCGGGGGCTCTTCTACCC`*, transcription from neural tube cDNA*). The vector for the *Lzts1* probe (pGEMT-Lzts1) was a kind gift from Dr. S. Wilson and the vector for the *Hes5.1* probe gifted by Dr. X. Morin.

Whole mount in situ hybridization

Embryos were fixed 2h at RT in 4% formaldehyde in PBS. Embryos were dehydrated with sequential washes in 50% ethanol/ PBS+ 0.1% Tween20 and 100% ethanol and conserved at -20°C. Embryos were bleached for 45mn in 80% ethanol + 20% H2O2-30% and then rehydrated. They were treated with proteinase K 10µg/ml at RT and refixed with 4% formaldehyde, 0.2% glutaraldehyde. After 1h of blocking in the hybridization buffer (50% formamide, SSC 5X, 50µg/mL Heparine, yeast tRNA 50µg/mL, SDS 1%) hybridization with DIG-labelled RNA probes (*HoxB2*, *HoxB4*, *HoxB7*, *HoxB8*, *HoxB9* and *Lzts1*) was performed at 68°C overnight. The next day, embryos were washed (3 times 30 minutes) in hybridization buffer and 1 time in TBS (25 mM Tris, 150 mM NaCl, 2 mM KCl, pH 7.4) +0.1% Tween 20.

They were incubated 1h at RT in a blocking buffer (20% Blocking reagent + 20% Goat serum) and then overnight with an anti-DIG-AP antibody (1:2000, Roche) in the blocking buffer. After 3 washes (1 hour) in TBS+0.1% Tween 20, embryos were equilibrated (2 times 10 minutes) in NTMT buffer (NaCl 100mM, TrisHCl 100mM pH9,5, MgCl2 50mM, 2%Tween20) and incubated in NBT/BCIP (Promega) at RT in the dark until color development. Pictures of whole embryos were made using a BinoFluo MZFLIII and a color camera.

RNA-seq analysis

Electroporations were carried out as described in a previous section but with 5 bilateral pulses. Plasmids DNA concentrations were for the control mix: pCIG 2µg/µl and for the HoxB8 mix: HoxB8-pCIG 1 µg/µl + pCIG 1µg/µl. Part of the neural tube expressing the GFP were dissected 18 hours after electroporation and dissociated (Trypsin-EDTA 0,25%). GFP and CDS take around 3 hours to be expressed after electroporation. As a consequence, 18 hours post-electroporation means that HoxB8 is overexpressed in neural tube cells for about 15 hours. We have chosen this timing as it is the earliest at which the size of the neural tube allows for rapid dissection, a condition required for collecting sufficient starting material for FACS in a minimum timeframe. A highly enriched population of GFP-expressing cells was isolated by FACS with the use of a dead cell exclusion (DCE)/discrimination dye (DAPI) to eliminate dying cells (Supplementary Fig. 8). RNA was extracted (RNeasy Mini Kit) and reverse transcribed and cDNA was amplified using a linear amplification system and used for sequencing library building (GATC): Random primed cDNA library, purification of poly-A containing mRNA molecules, mRNA fragmentation, random primed cDNA synthesis, adapter ligation and adapter specific PCR amplification, Illumina technology, 50 000 000 reads paired end with 2 x 50 bp read length. Bioinformatics analysis were done using the galgal4.0 chicken genome. Qualitative analysis of RNA-seq data from the two biological replicates shows a high Pearson Correlation score (>0,98) indicative of the experimental reproducibility (Supplementary Fig. 9).

RNA-seq data have been deposited in NCBI's Gene Expression Omnibus and are accessible through GEO Series access number GSE162665.

Quantifications and statistical significance

The number of embryos and number sections analyzed are indicated in the figure legends. A minimum of 3 embryos and 6 sections per embryos were used to quantify. All quantifications

were made using the cell counter tool of Fiji software. The results were analyzed and plotted using Prism 8 software (GraphPad software). Statistical analyses were performed using a two-tailed Mann Whitney test and considered significant when p-value < 0,05. All p-values are indicated on the graphs. The error bars represent the standard deviation (SD).

Acknowledgements

We thank Olivier Pourquié, Jeremy Dasen, Xavier Morin, Heather Etchevers and Sara Wilson for their generous gifts of antibodies, RNA probes and/or expression vectors. We sincerely thank Samuel Tozer, Heather Etchevers and Xavier Morin for critical reading of the manuscript. FACS experiments were done at the CRCM (Marseille, France).

Competing interests

The authors declare no competing or financial interests.

Funding

This work was supported by AMIDEX and the FRM. Axelle Wilmerding and Lucrezia Rinaldi were respectively funded by doctoral fellowships from LA LIGUE CONTRE LE CANCER and AMIDEX.

FIGURE LEGENDS

Figure 1: *HoxB* genes are expressed in the trunk neural tube during early neurogenesis with little antero-posterior axial specificity

A- *HoxB2*, *HoxB4*, *HoxB7*, *HoxB8* and *HoxB9* gene expression patterns of E3 chicken embryos by whole mount *in situ* hybridization. **B-** Schematic of *HoxB* gene (except *HoxB13*) expression patterns at E3 in the trunk neural tube showing overlapping patterns from the neck (with little spatial collinearity) to the tail. **C-** Brachial and thoracic HoxB9 and HoxC9 protein expression patterns at E3, E4 and E5 by immunofluorescence on transversal sections. In the trunk neural tube, HoxB9 protein is expressed as early as E3 and is excluded from the motor neuron territories at E4. Its paralog protein HoxC9 is expressed from E4 in the motor neuron territories. **D-** HoxB9 and HoxC9 protein expression patterns along the neural tube at E5. HoxB9 protein is expressed all along the trunk neural tube. Its paralog HoxC9 is only expressed at the thoracic level. **E-** Immunofluorescences and fluorescent *in situ* hybridizations (FISH) of HoxB9 protein (green), *HoxB8* gene (red) and Hoechst (nuclear staining, blue) show a strong expression overlap in the neural tube at E4.5 between a posterior and a central HoxB gene (Scale bar: 50µm).

Figure 2: *HoxB* genes are expressed in the IZ and their gain-of-function leads to ectopic progenitor cells in the MZ

A- Immunofluorescences and FISH on transversal sections of trunk neural tube at E4. The expression of Sox2 and Tuj1 (respectively markers of the VZ (progenitors) and the MZ (neurons) in green and blue) and expression of the *NeuroD4* gene (marker of the IZ, in red) illustrate that *HoxB9* is mainly expressed in the IZ. **B-** Immunofluorescences on transversal sections three days after electroporation of the chicken neural tube with a control (pCAGGS), HoxB4, HoxB8 or HoxB9 expression vectors (in the pCAGGS vector), co-transfected with a vector expressing the cell death inhibitor P35, stained with GFP (green), Tuj1 (red) and Sox2 (blue) antibodies. The gain-of-function in all three cases leads to the appearance of ectopic positive Sox2 cells in the MZ. **C-** Percentage of ectopic Sox2+ cells among the GFP+ cells in the MZ per section, three days after co-electroporation of a vector expressing P35 and the

control pCAGGS (n= 3 animals / 18 sections) or Hox expressing pCAGGS vectors (HoxB4 (n= 3 animals/ 21 sections), HoxB8 (n= 3 animals/ 21 sections) and HoxB9 (n= 3 animals/ 19 sections) (in +P35 condition). The quantifications showed a significant increase of ectopic Sox2 cells in the MZ after any HoxB gain-of-function. (Two-tailed Mann-Whitney test, error bars represent SD). **D-** High magnification of immunofluorescences on transversal sections in the MZ three days after electroporation of the chicken neural tube with HoxB8 +P35 vectors, stained with GFP (green), Sox2 (red), and Hoechst (blue), illustrating that while most Sox2 ectopic cells are GFP+, some ectopic Sox2+ cells in the MZ are also GFP- (white arrow, top panel). Staining with a mitotic marker pH3 (s28) (magenta) (in the bottom panel) identifies HoxB8-induced Sox2+ cells in the MZ, indicating that these cells are still mitotic (Sox2+ and pH3+, white border arrow on all three panels) (Scale bar: 50µm).

Figure 3: Identification of *Lzts1*, expressed in the IZ, as a HoxB8 downstream target by RNAseq analysis

A- 18h after bilateral electroporation of trunk neural tube at the stage HH12 with the pCIG control vector (expression of GFP only) or the pCIG-HoxB8 (expression of GFP and HoxB8), the electroporated region of the neural tube was dissected (18 to 20 embryos per condition in duplicates) and the GFP+ cells were sorted by FACS. **B-** Volcano plot of Differential Gene Expression (DGE) for the HoxB8 versus control (pCIG) conditions. The position of *Lzts1* in the volcano plot is circled. (FDR: False Discovery Rate; FC: Fold Change). **C-** Circle graphs representing the number of HoxB8 up-regulated and down-regulated genes for a FDR=5 (all the genes) or for a FDR=5 and a FC>2. This illustrates that HoxB8 acts more as an activator than a repressor of transcription. **D-** Gene ontology enrichment analysis (GOEA) of the biological processes for up (top table) and downregulated genes (low table). This analysis suggests a HoxB8 pleiotropic function during spinal cord development **E-** The graph of the number of *Lzts1* TPM (Transcripts Per Kilobase Million) obtained for the two replicates of the control (pCIG1, pCIG2) and HoxB8 (HoxB8-1 and HoxB8-2) expressing samples, illustrates the reproducibility between replicates.

Figure 4: *Lzts1* expression in the IZ is controlled by *HoxB* genes

A- FISH on trunk transversal sections of chicken embryo at E3 with *Lzts1* probe. **B-** FISH and immunofluorescences on trunk transversal sections of chicken embryo at E4 showing an overlapping expression of *Lzts1* gene (red) and HoxB9 protein (green) in the IZ. **C-** The gain-of-function of HoxB4, HoxB8 or HoxB9 two days after electroporation (GFP, green) induces

the ectopic expression of *Lzts1* (red) in the VZ. Blue is Hoechst staining. Arrows point *Lzts1* ectopic expression. (Scale bar: 50µm).

Figure 5: *Lzts1* gain-of-function triggers neuronal delamination and leads to ectopic progenitor cells in the MZ

A- Lzts1 gain-of-function induces massive delamination of the electroporated cells two and three days following electroporation. Cells electroporated with a control vector (pCAGGS) do not display this phenotype. **B-** The gain-of-function of Lzts1, two and three days after electroporation induces ectopic Sox2 positive cells in the MZ. **C-** Percentage of ectopic Sox2+ cells among the GFP+ cells in the MZ per section. Counts performed three days after the electroporation for control plasmids pCIG or pCAGGS (n= 3 animals / 18 sections) or Lzts1 expressing plasmid (n= 3 animals / 18 sections) showed a significant and strong increase of ectopic Sox2 cells in the MZ (Two-tailed Mann-Whitney test, error bars represent SD). **D-E-F-G-** FISH and/or immunofluorescences on transversal sections of trunk neural tube two or three days after the Lzts1 expressing vector electroporation. Lzts1 induces the presence of ectopic *CCND1*, pH3, *Hes5.1* and *NeuroD4* expressing cells in the MZ. (GFP, green and Hoechst, blue, scale bar: 50µm).

Figure 6: *Lzts1* loss-of-function inhibits neuronal delamination downstream of HoxB8

A- FISH on trunk transversal sections stained for *Lzts1* transcripts (green) two days after electroporation of a ShRNA-Lzts1 expression plasmid (co-expressing RFP) shows a reduction in the quantity of *Lzts1* transcripts. **B-** Electroporation of ShRNA-Lzts1 does not lead to Sox2 ectopic expression. **C-F-** Knock-down of *Lzts1* (ShRNA-Lzts1) while inhibiting cell death (co-electroporation with a P35 expressing vector) leads to ectopic Tuj1 (membrane) and Huc/D (cytoplasmic) expression, neuronal markers in the VZ, with neurons still attached to the apical surface (RFP, red and Hoechst, blue). The number of Tuj1 protrusions (**D**) and ectopic Huc/D cells (**F**) in the VZ per section were quantified two days after the electroporation (n=3 animals / 41 sections-Tuj1 and 35 sections-HuC/D), and compared to a control experiment (ShRNA-scramble (scr) + P35; n=3 animals / 42 slides-Tuj1 and 24 slides-HuC/D). (Two-tailed Mann-Whitney test, error bars represent SD). **G-H-I-** Co-expression of HoxB8 with ShRNA-Lzts1 (in the P35 context) leads to less Sox2 ectopic cells in the MZ compared to HoxB8 co-expressed with the scramble ShRNA (RFP, red, GFP, green and Hoechst, blue, scale bar 50µm). The percentage of ectopic Sox2+ cells among the GFP+ cells in the MZ was counted two days after the electroporation of ShRNA-scramble + HoxB8 +

P35 (n= 3 animals / 32 sections) and shRNA-Lzts1 + HoxB8 + P35 (n= 3 animals / 38 sections) (Two-tailed Mann-Whitney test, error bars represent SD).

Figure 7: Model

A- During the developing spinal cord, non-HoxB proteins start to be expressed in the trunk neural tube at E4 and are expressed in a clear antero-posterior spatial collinear manner, and mainly in the motor neurons territories. **B-** HoxB proteins (except HoxB13) are expressed during early neurogenesis (from E3), present poor antero-posterior spatial collinearity (largely overlapping expression from neck to tail. They are not expressed in motor neuron territories but preferentially expressed in the IZ at E4. The data presented in this study show that HoxB proteins control *Lzts1* expression in the IZ which controls neuronal delamination (B).

REFERENCES

Asli, N. S. and Kessel, M. (2010). Spatiotemporally restricted regulation of generic motor neuron programs by miR-196-mediated repression of Hoxb8. *Dev. Biol.* **344**, 857–868.

Baek, C., Freem, L., Goïame, R., Sang, H., Morin, X. and Tozer, S. (2018). Mib1 prevents Notch Cis-inhibition to defer differentiation and preserve neuroepithelial integrity during neural delamination. *PLoS Biol.* **16**, e2004162.

Baffa, R., Fassan, M., Sevignani, C., Vecchione, A., Ishii, H., Giarnieri, E., Iozzo, R. V., Gomella, L. G. and Croce, C. M. (2008). Fez1/Lzts1-deficient mice are more susceptible to N-butyl-N-(4-hydroxybutil) nitrosamine (BBN) carcinogenesis. *Carcinogenesis* **29**, 846–848.

Banreti, A., Hudry, B., Sass, M., Saurin, A. J. and Graba, Y. (2014). Hox proteins mediate developmental and environmental control of autophagy. *Dev. Cell* **28**, 56–69.

Bel-Vialar, S., Itasaki, N. and Krumlauf, R. (2002). Initiating Hox gene expression: in the early chick neural tube differential sensitivity to FGF and RA signaling subdivides the HoxB genes in two distinct groups. *Dev. Camb. Engl.* **129**, 5103–5115.

Bertrand, N., Castro, D. S. and Guillemot, F. (2002). Proneural genes and the specification of neural cell types. *Nat. Rev. Neurosci.* **3**, 517–530.

Corral, R. D. del and Storey, K. G. (2001). Markers in vertebrate neurogenesis. *Nat. Rev. Neurosci.* **2**, 835–839.

Crawford, M. (2003). Hox genes as synchronized temporal regulators: Implications for morphological innovation. *J. Exp. Zool.* **295B**, 1–11.

Das, R. M., Van Hateren, N. J., Howell, G. R., Farrell, E. R., Bangs, F. K., Porteous, V. C., Manning, E. M., McGrew, M. J., Ohyama, K., Sacco, M. A., et al. (2006). A robust system for RNA interference in the chicken using a modified microRNA operon. *Dev. Biol.* **294**, 554–563.

Dasen, J. S., Liu, J.-P. and Jessell, T. M. (2003). Motor neuron columnar fate imposed by sequential phases of Hox-c activity. *Nature* **425**, 926–933.

Dasen, J. S., Tice, B. C., Brenner-Morton, S. and Jessell, T. M. (2005). A Hox Regulatory Network Establishes Motor Neuron Pool Identity and Target-Muscle Connectivity. *Cell* **123**, 477–491.

Dasen, J. S., De Camilli, A., Wang, B., Tucker, P. W. and Jessell, T. M. (2008). Hox Repertoires for Motor Neuron Diversity and Connectivity Gated by a Single Accessory Factor, FoxP1. *Cell* **134**, 304–316.

Denans, N., Iimura, T. and Pourquié, O. (2015). Hox genes control vertebrate body elongation by collinear Wnt repression. *eLife* **4**, e04379.

Duboule, D. (2007). The rise and fall of Hox gene clusters. *Development* **134**, 2549–2560.

Duboule, D. and Dollé, P. (1989). The structural and functional organization of the murine HOX gene family resembles that of Drosophila homeotic genes. *EMBO J.* **8**, 1497–1505.

Fior, R. and Henrique, D. (2005). A novel hes5/hes6 circuitry of negative regulation controls Notch activity during neurogenesis. *Dev. Biol.* **281**, 318–333.

Fishwick, K. J., Li, R. A., Halley, P., Deng, P. and Storey, K. G. (2010). Initiation of neuronal differentiation requires PI3-kinase/TOR signalling in the vertebrate neural tube. *Dev. Biol.* **338**, 215–225.

Formosa-Jordan, P., Ibañes, M., Ares, S. and Frade, J.-M. (2013). Lateral inhibition and neurogenesis: novel aspects in motion. *Int. J. Dev. Biol.* **57**, 341–350.

Garcia-Gutierrez, P., Juarez-Vicente, F., Wolgemuth, D. J. and Garcia-Dominguez, M. (2014). Pleiotrophin antagonizes Brd2 during neuronal differentiation. *J. Cell Sci.* **127**, 2554–2564.

Götz, M. and Huttner, W. B. (2005). The cell biology of neurogenesis. *Nat. Rev. Mol. Cell Biol.* **6**, 777–788.

Graham, A., Maden, M. and Krumlauf, R. (1991). The murine Hox-2 genes display dynamic dorsoventral patterns of expression during central nervous system development. *Dev. Camb. Engl.* **112**, 255–264.

Hamburger, V. and Hamilton, H. L. (1992). A series of normal stages in the development of the chick embryo. *Dev. Dyn.* **195**, 231–272.

Hatakeyama, J. (2004). Hes genes regulate size, shape and histogenesis of the nervous system by control of the timing of neural stem cell differentiation. *Development* **131**, 5539–5550.

Hatakeyama, J., Sakamoto, S. and Kageyama, R. (2006). *Hes1* and *Hes5* Regulate the Development of the Cranial and Spinal Nerve Systems. *Dev. Neurosci.* **28**, 92–101.

Hayashi, S. and Scott, M. P. (1990). What determines the specificity of action of Drosophila homeodomain proteins? *Cell* **63**, 883–894.

He, Y. and Liu, X. (2015). The tumor-suppressor gene LZTS1 suppresses hepatocellular carcinoma proliferation by impairing PI3K/Akt pathway. *Biomed. Pharmacother. Biomedecine Pharmacother.* **76**, 141–146.

Iimura, T. and Pourquié, O. (2006). Collinear activation of Hoxb genes during gastrulation is linked to mesoderm cell ingression. *Nature* **442**, 568–571.

Ishii, H., Baffa, R., Numata, S. I., Murakumo, Y., Rattan, S., Inoue, H., Mori, M., Fidanza, V., Alder, H. and Croce, C. M. (1999). The FEZ1 gene at chromosome 8p22 encodes a leucine-zipper protein, and its expression is altered in multiple human tumors. *Proc. Natl. Acad. Sci. U. S. A.* **96**, 3928–3933.

Ishii, H., Vecchione, A., Murakumo, Y., Baldassarre, G., Numata, S., Trapasso, F., Alder, H., Baffa, R. and Croce, C. M. (2001). FEZ1/LZTS1 gene at 8p22 suppresses cancer cell growth and regulates mitosis. *Proc. Natl. Acad. Sci. U. S. A.* **98**, 10374–10379.

Jung, H., Lacombe, J., Mazzoni, E. O., Liem, K. F., Grinstein, J., Mahony, S., Mukhopadhyay, D., Gifford, D. K., Young, R. A., Anderson, K. V., et al. (2010). Global control of motor neuron topography mediated by the repressive actions of a single hox gene. *Neuron* **67**, 781–796.

Kasioulis, I. and Storey, K. G. (2018). Cell biological mechanisms regulating chick neurogenesis. *Int. J. Dev. Biol.* **62**, 167–175.

Kawaue, T., Shitamukai, A., Nagasaka, A., Tsunekawa, Y., Shinoda, T., Saito, K., Terada, R., Bilgic, M., Miyata, T., Matsuzaki, F., et al. (2019). Lzts1 controls both neuronal delamination and outer radial glial-like cell generation during mammalian cerebral development. *Nat. Commun.* **10**, 2780.

Kropp, M. and Wilson, S. I. (2012). The expression profile of the tumor suppressor gene Lzts1 suggests a role in neuronal development. *Dev. Dyn. Off. Publ. Am. Assoc. Anat.* **241**, 984–994.

Lacombe, J., Hanley, O., Jung, H., Philippidou, P., Surmeli, G., Grinstein, J. and Dasen, J. S. (2013). Genetic and functional modularity of Hox activities in the specification of limb-innervating motor neurons. *PLoS Genet.* **9**, e1003184.

Lacomme, M., Liaubet, L., Pituello, F. and Bel-Vialar, S. (2012). NEUROG2 drives cell cycle exit of neuronal precursors by specifically repressing a subset of cyclins acting at the G1 and S phases of the cell cycle. *Mol. Cell. Biol.* **32**, 2596–2607.

Le Dréau, G. and Martí, E. (2012). Dorsal-ventral patterning of the neural tube: a tale of three signals. *Dev. Neurobiol.* **72**, 1471–1481.

Lee, H. O. and Norden, C. (2013). Mechanisms controlling arrangements and movements of nuclei in pseudostratified epithelia. *Trends Cell Biol.* **23**, 141–150.

Luo, L., Yang, X., Takihara, Y., Knoetgen, H. and Kessel, M. (2004). The cell-cycle regulator geminin inhibits Hox function through direct and polycomb-mediated interactions. *Nature* **427**, 749–753.

Ma, Q., Kintner, C. and Anderson, D. J. (1996). Identification of neurogenin, a vertebrate neuronal determination gene. *Cell* **87**, 43–52.

Mann, R. S. and Chan, S. K. (1996). Extra specificity from extradenticle: the partnership between HOX and PBX/EXD homeodomain proteins. *Trends Genet. TIG* **12**, 258–262.

Mann, R. S., Lelli, K. M. and Joshi, R. (2009). Hox specificity unique roles for cofactors and collaborators. *Curr. Top. Dev. Biol.* **88**, 63–101.

Merabet, S. and Mann, R. S. (2016). To Be Specific or Not: The Critical Relationship Between Hox And TALE Proteins. *Trends Genet. TIG* **32**, 334–347.

Patterson, E. S., Waller, L. E. and Kroll, K. L. (2014). Geminin loss causes neural tube defects through disrupted progenitor specification and neuronal differentiation. *Dev. Biol.* **393**, 44–56.

Pearson, J. C., Lemons, D. and McGinnis, W. (2005). Modulating Hox gene functions during animal body patterning. *Nat. Rev. Genet.* **6**, 893–904.

Philippidou, P. and Dasen, J. S. (2013). Hox genes: choreographers in neural development, architects of circuit organization. *Neuron* **80**, 12–34.

Rezsohazy, R., Saurin, A. J., Maurel-Zaffran, C. and Graba, Y. (2015). Cellular and molecular insights into Hox protein action. *Dev. Camb. Engl.* **142**, 1212–1227.

Rinaldi, L., Saurin, A. J. and Graba, Y. (2018). Fattening the perspective of Hox protein specificity through SLiMming. *Int. J. Dev. Biol.* **62**, 755–766.

Sahdev, S., Saini, K. S. and Hasnain, S. E. (2010). Baculovirus P35 protein: an overview of its applications across multiple therapeutic and biotechnological arenas. *Biotechnol. Prog.* **26**, 301–312.

Saurin, A. J., Delfini, M. C., Maurel-Zaffran, C. and Graba, Y. (2018). The Generic Facet of Hox Protein Function. *Trends Genet.* **34**, 941–953.

Sweeney, L. B., Bikoff, J. B., Gabitto, M. I., Brenner-Morton, S., Baek, M., Yang, J. H., Tabak, E. G., Dasen, J. S., Kintner, C. R. and Jessell, T. M. (2018). Origin and Segmental Diversity of Spinal Inhibitory Interneurons. *Neuron* **97**, 341-355.e3.

Vecchione, A., Baldassarre, G., Ishii, H., Nicoloso, M. S., Belletti, B., Petrocca, F., Zanesi, N., Fong, L. Y. Y., Battista, S., Guarnieri, D., et al. (2007). Fez1/Lzts1 absence impairs Cdk1/Cdc25C interaction during mitosis and predisposes mice to cancer development. *Cancer Cell* **11**, 275–289.

Vilas-Boas, F. and Henrique, D. (2010). HES6-1 and HES6-2 function through different mechanisms during neuronal differentiation. *PloS One* **5**, e15459.

Zandvakili, A. and Gebelein, B. (2016). Mechanisms of Specificity for Hox Factor Activity. *J. Dev. Biol.* **4**,.

Zhou, W., He, M.-R., Jiao, H.-L., He, L.-Q., Deng, D.-L., Cai, J.-J., Xiao, Z.-Y., Ye, Y.-P., Ding, Y.-Q., Liao, W.-T., et al. (2015). The tumor-suppressor gene LZTS1 suppresses colorectal cancer proliferation through inhibition of the AKT-mTOR signaling pathway. *Cancer Lett.* **360**, 68–75.

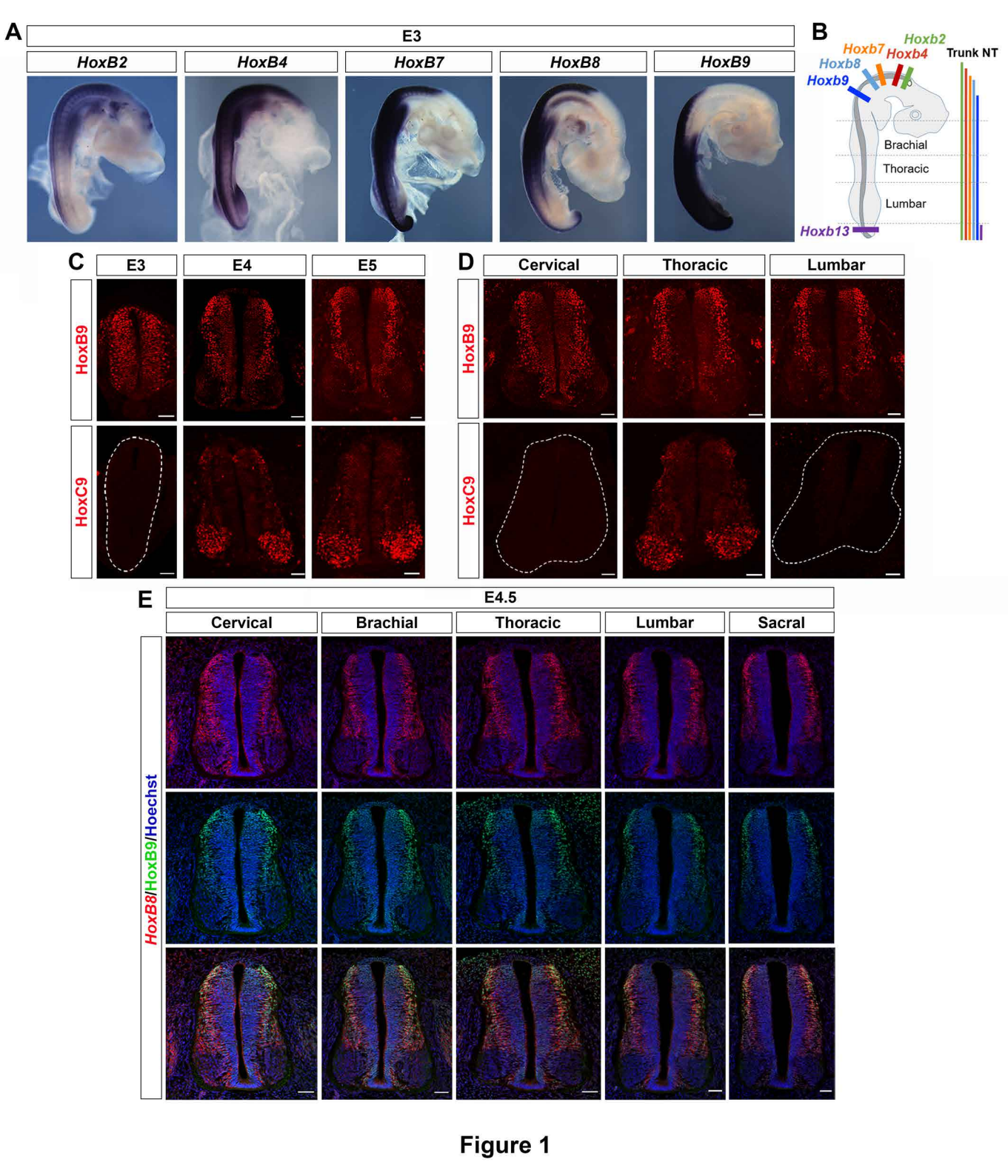
A
E3
HoxB2
HoxB4
HoxB7
HoxB8
HoxB9
B
Hoxb2
Hoxb7
Hoxb4
Hoxb8
Hoxb9
Trunk NT
Brachial
Thoracic
Lumbar
Hoxb13
C
E3
E4
E5
HoxB9
HoxC9
D
Cervical
Thoracic
Lumbar
HoxB9
HoxC9
E
E4.5
Cervical
Brachial
Thoracic
Lumbar
Sacral
HoxB8/HoxB9/Hoechst

Figure 1

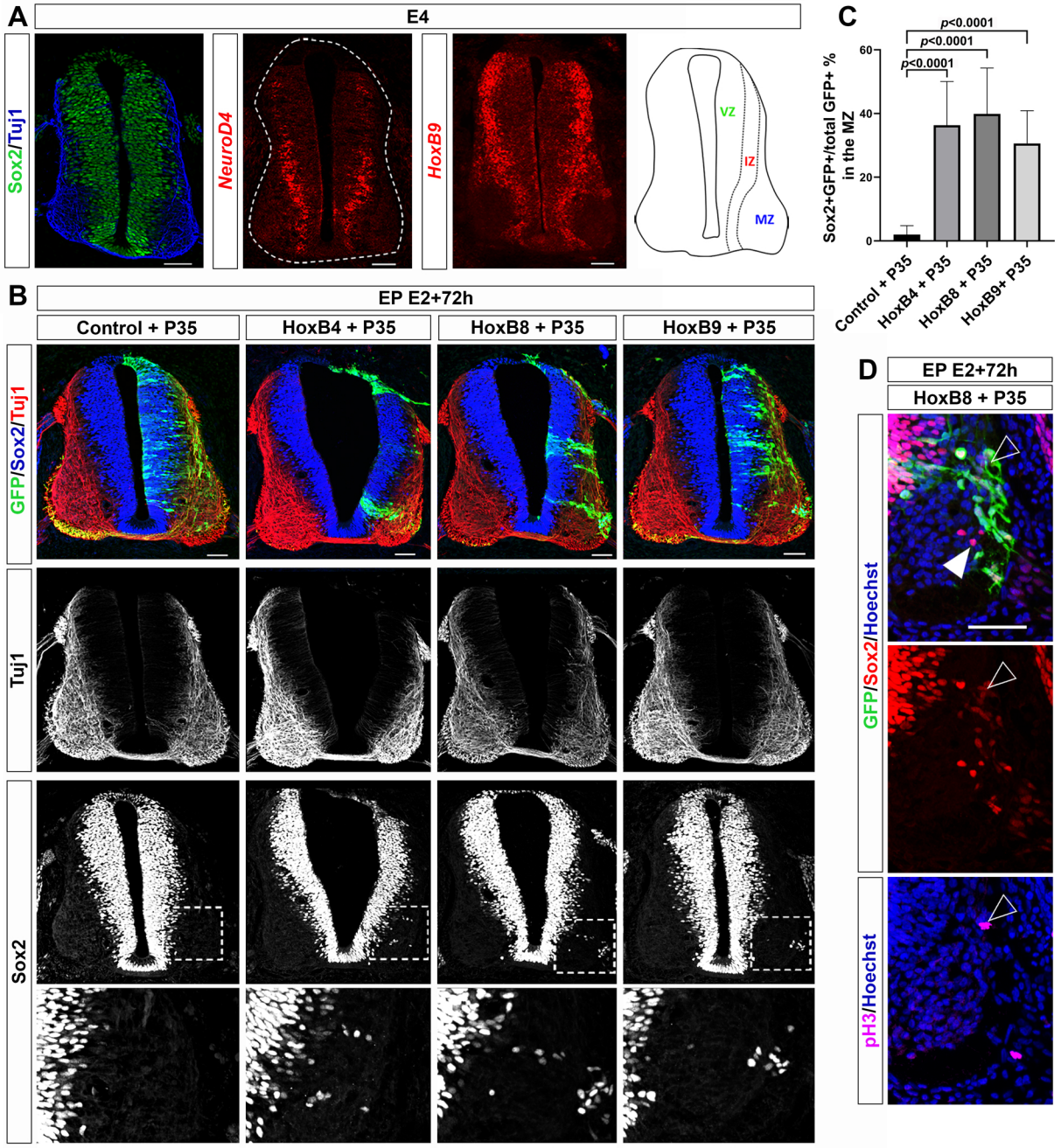
A
E4
Sox2/Tuj1
NeuroD4
HoxB9
VZ
IZ
MZ
C
p<0.0001
p<0.0001
p<0.0001
Sox2+GFP+/total GFP+ % in the MZ
60
40
20
0
Control + P35
HoxB4 + P35
HoxB8 + P35
HoxB9+ P35
B
EP E2+72h
Control + P35
HoxB4 + P35
HoxB8 + P35
HoxB9 + P35
GFP/Sox2/Tuj1
Tuj1
Sox2
D
EP E2+72h
HoxB8 + P35
GFP/Sox2/Hoechst
pH3/Hoechst

Figure 2

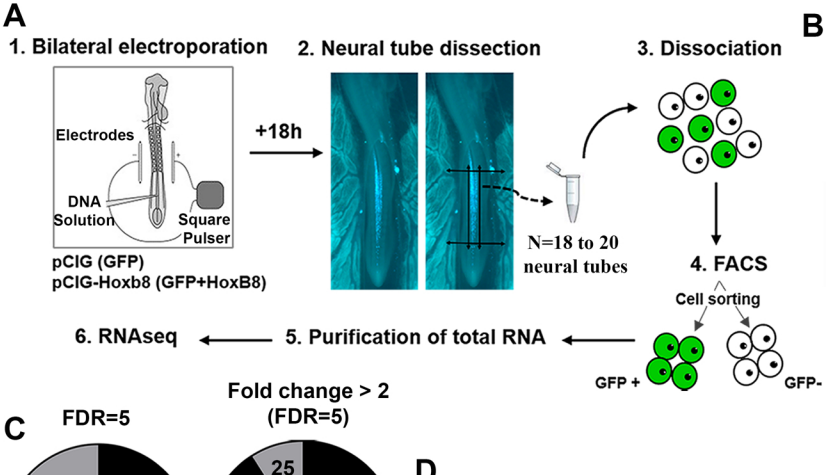

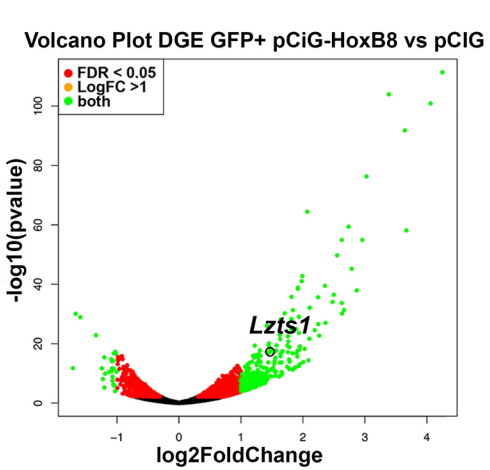

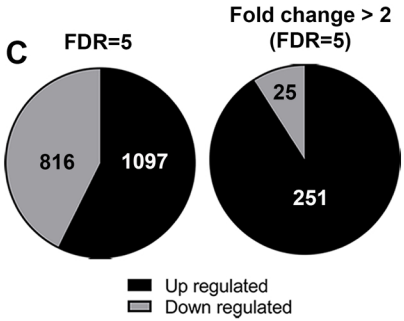

D

GOEA biological process complete - HoxB8/PCIG upregulated genes	Fold Enrichment	P value
Regulation of signaling	1.64	1.29E-09
Regulation of cell communication	1.61	8.70E-09
Neuron differentiation	1.99	7.40E-07
Regulation of cell migration	2.12	2.00E-06
Transmembrane receptor protein tyrosine kinase signaling pathway	2.54	6.09E-06
Movement of cell or subcellular component	1.75	7.46E-06
Positive regulation of Wnt signaling pathway	3.40	9.73E-05
Positive regulation of catalytic activity	1.65	1.03E-04
Regulation of plasma membrane bounded cell projection organization	2.01	1.25E-04
Regulation of cell adhesion	1.93	4.60E-04

GOEA biological process complete - HoxB8/PCIG downregulated genes	Fold Enrichment	P value
Ribonucleoprotein complex biogenesis	4.18	1.63E-15
Morphogenesis of an epithelium	3.14	8.44E-08
Neural tube formation	5.14	5.10E-06
Anterior/posterior pattern specification	3.30	8.53E-06
Regulation of neuron differentiation	2.36	1.17E-05
Negative regulation of apoptotic process	2.27	1.26E-05
Cell cycle checkpoint	3.72	3.30E-05
Chromatin assembly or disassembly	4.14	1.56E-04
Notch signaling pathway	4.22	2.68E-04
Movement of cell or subcellular component	1.64	5.48E-04

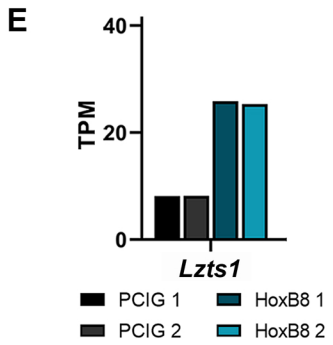

Figure 3

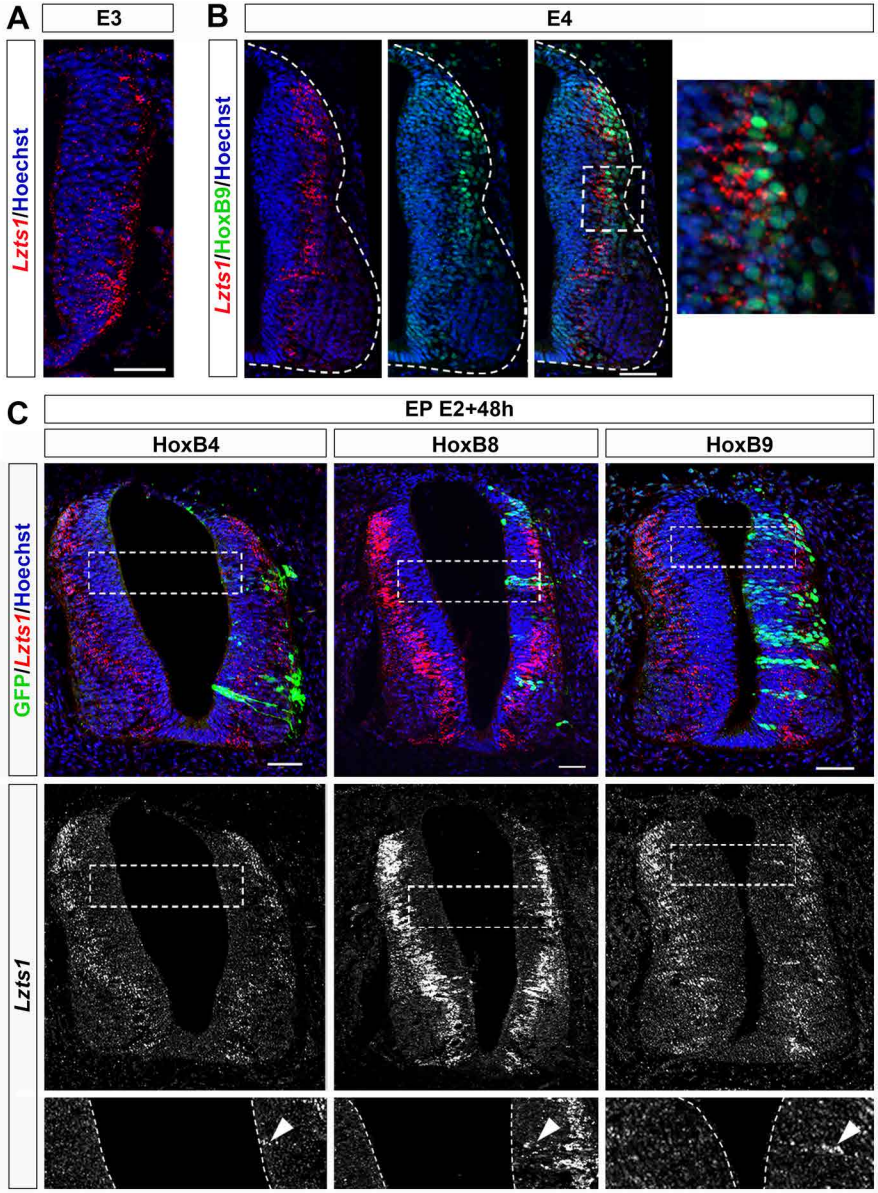
A
E3
Lzts1/Hoechst
B
E4
Lzts1/HoxB9/Hoechst
C
EP E2+48h
HoxB4
HoxB8
HoxB9
GFP/Lzts1/Hoechst
Lzts1

Figure 4

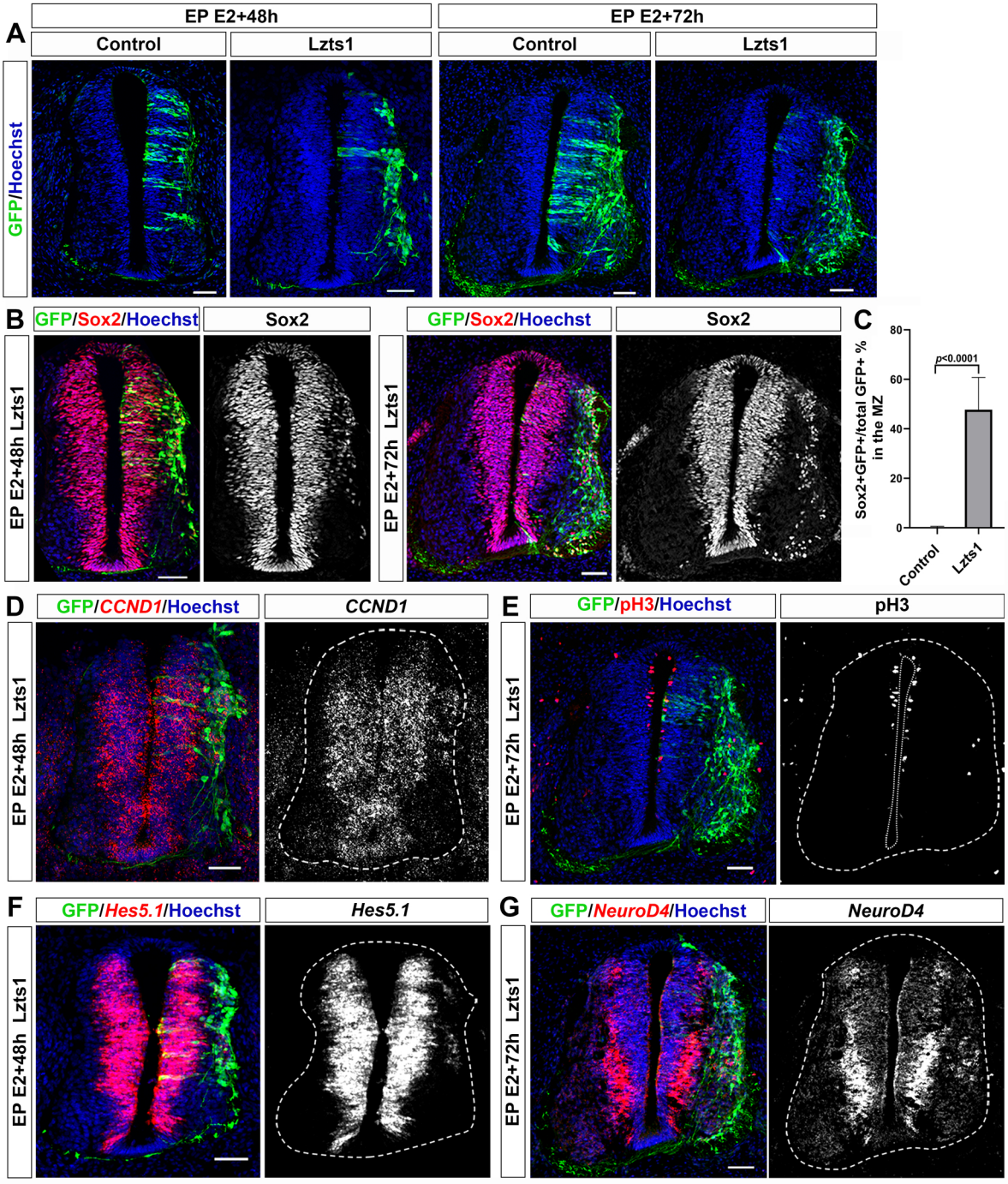
A
EP E2+48h
EP E2+72h
Control
Lzts1
Control
Lzts1
GFP/Hoechst
B
GFP/Sox2/Hoechst
Sox2
GFP/Sox2/Hoechst
Sox2
EP E2+48h Lzts1
EP E2+72h Lzts1
C
Sox2+GFP+/total GFP+ % in the MZ
p<0.0001
80
60
40
20
0
Control
Lzts1
D
GFP/CCND1/Hoechst
CCND1
EP E2+48h Lzts1
E
GFP/pH3/Hoechst
pH3
EP E2+72h Lzts1
F
GFP/Hes5.1/Hoechst
Hes5.1
EP E2+48h Lzts1
G
GFP/NeuroD4/Hoechst
NeuroD4
EP E2+72h Lzts1

Figure 5

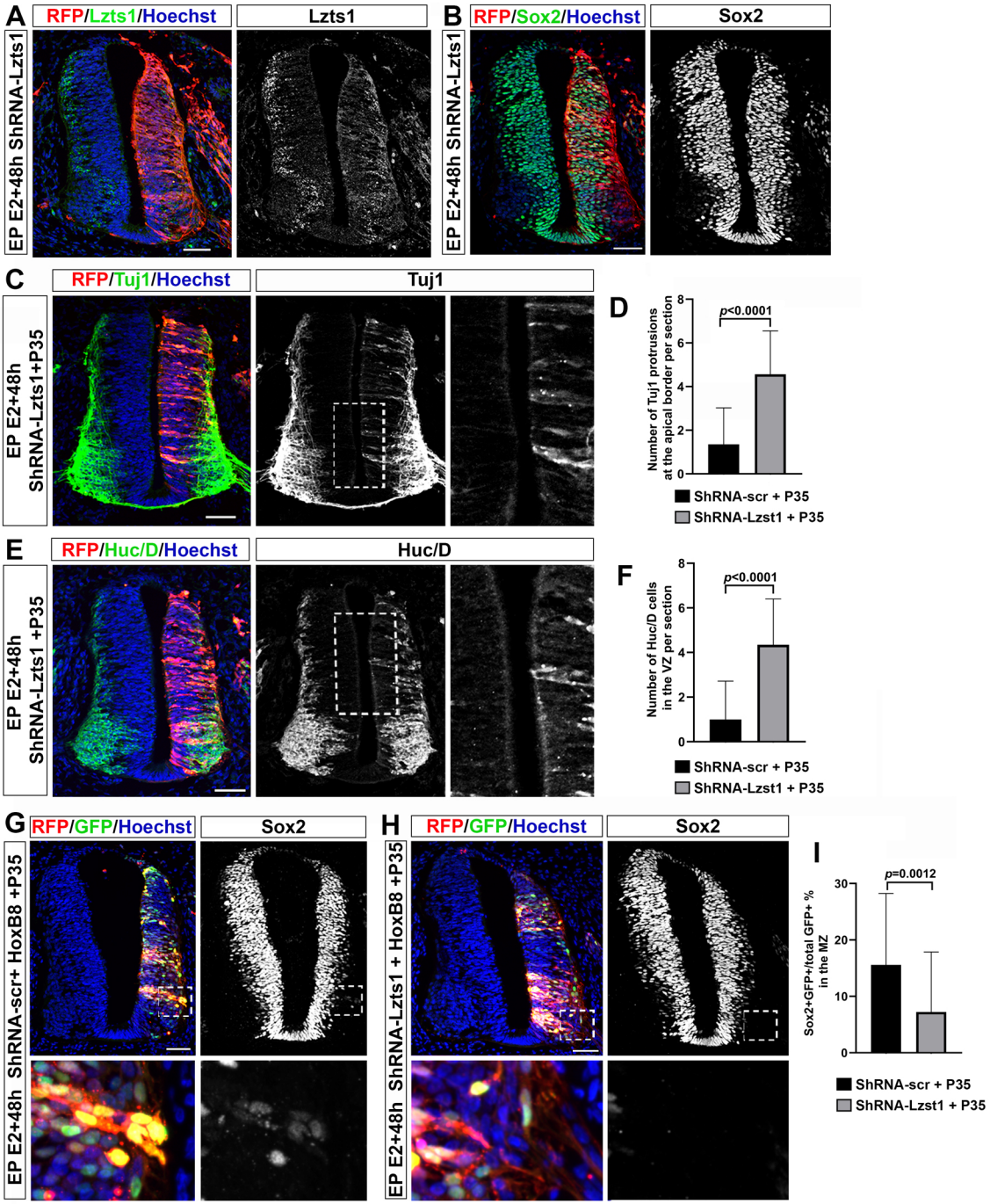
A
RFP/Lzts1/Hoechst
Lzts1
EP E2+48h ShRNA-Lzts1
B
RFP/Sox2/Hoechst
Sox2
EP E2+48h ShRNA-Lzts1
C
RFP/Tuj1/Hoechst
Tuj1
EP E2+48h ShRNA-Lzts1+P35
D
Number of Tuj1 protrusions at the apical border per section
p<0.0001
ShRNA-scr + P35
ShRNA-Lzst1 + P35
E
RFP/Huc/D/Hoechst
Huc/D
EP E2+48h ShRNA-Lzts1 +P35
F
Number of Huc/D cells in the VZ per section
p<0.0001
ShRNA-scr + P35
ShRNA-Lzst1 + P35
G
RFP/GFP/Hoechst
Sox2
EP E2+48h ShRNA-scr+ HoxB8 +P35
H
RFP/GFP/Hoechst
Sox2
EP E2+48h ShRNA-Lzts1 + HoxB8 +P35
I
Sox2+GFP+/total GFP+ % in the MZ
p=0.0012
ShRNA-scr + P35
ShRNA-Lzst1 + P35

Figure 6

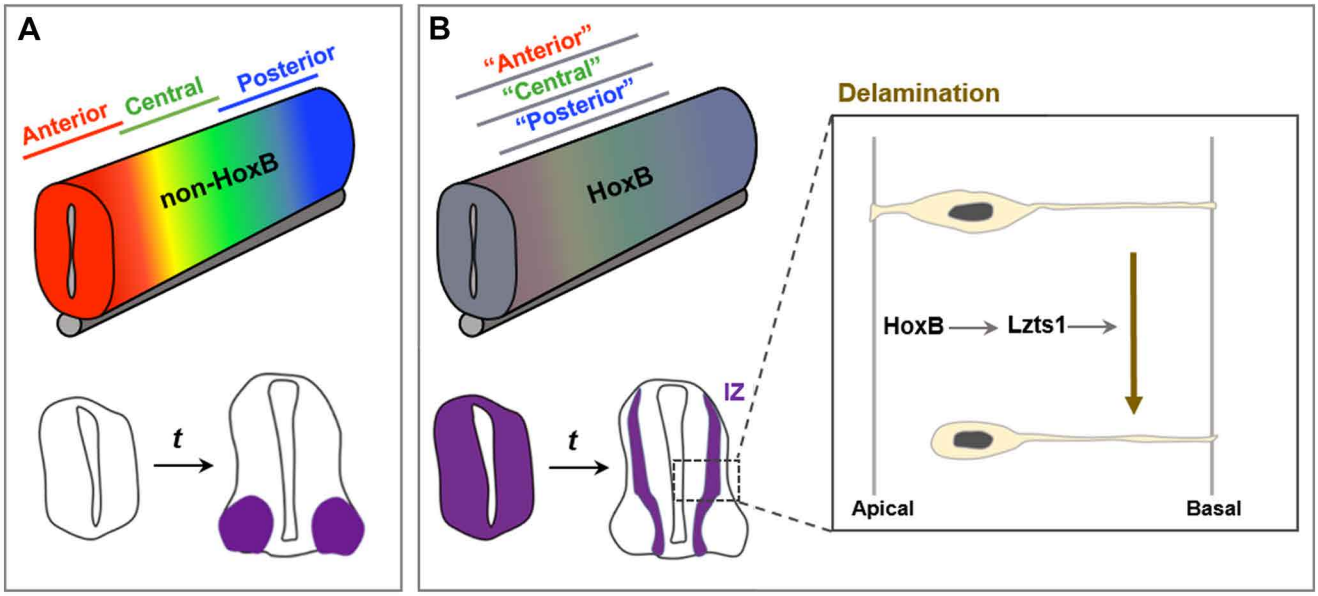
A
Anterior
Central
Posterior
non-HoxB
t
B
"Anterior"
"Central"
"Posterior"
HoxB
t
IZ
Delamination
HoxB
Lzts1
Apical
Basal

Figure 7